Molecular Cell, Volume *81*

Supplemental information

Alternative splicing is a developmental switch for hTERT expression

Alex Penev, Andrew Bazley, Michael Shen, Jef D. Boeke, Sharon A. Savage, and Agnel Sfeir

Supplemental Items:

Figure S1

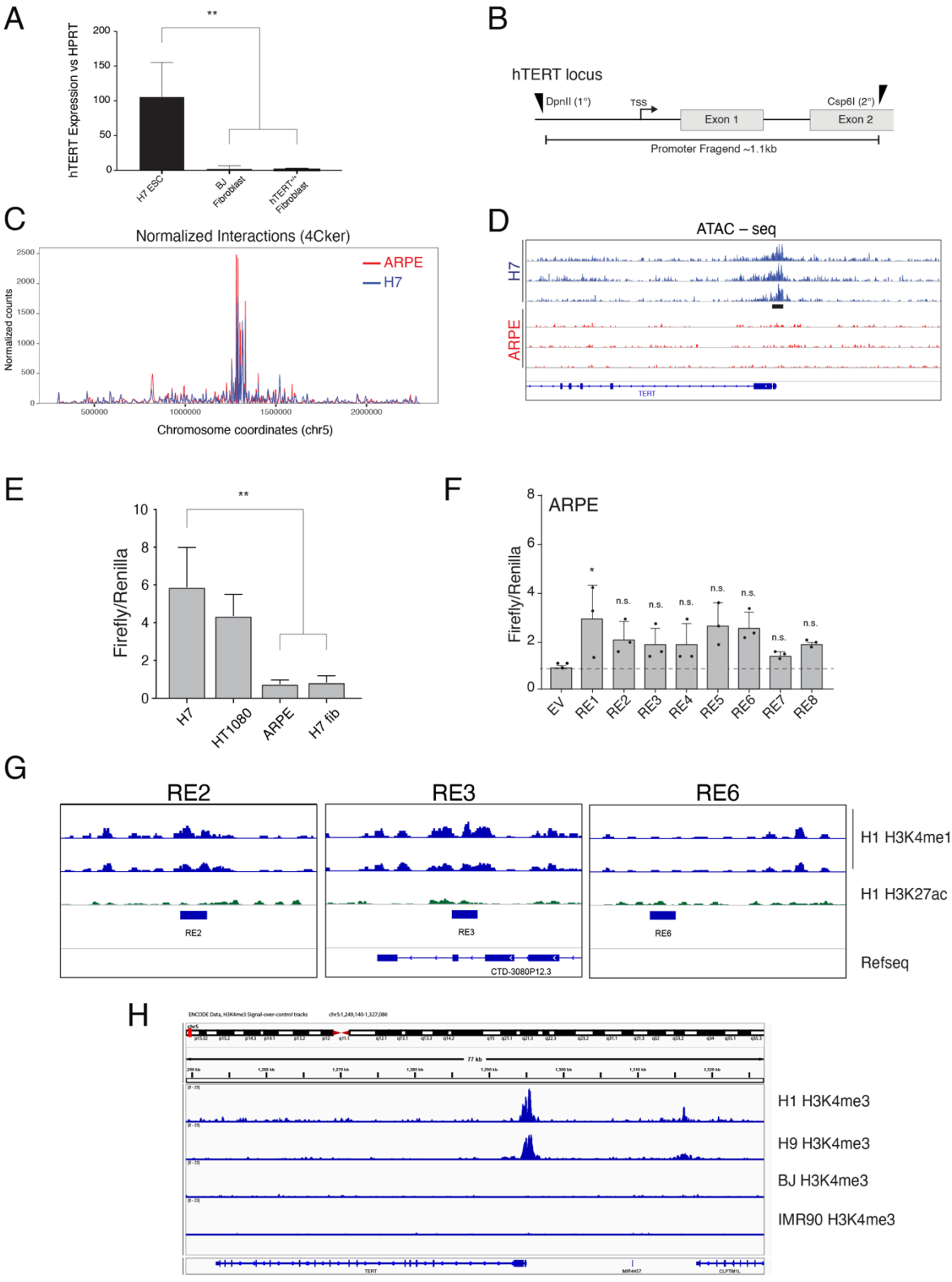
A
hTERT Expression vs HPRT
200
150
100
50
0
**
H7 ESC
BJ Fibroblast
hTERT+/+ Fibroblast
B
hTERT locus
DpnII (1°)
TSS
Csp6I (2°)
Exon 1
Exon 2
Promoter Fragend ~1.1kb
C
Normalized Interactions (4Cker)
ARPE
H7
Normalized counts
2500
2000
1500
1000
500
0
500000
1000000
1500000
2000000
Chromosome coordinates (chr5)
D
ATAC – seq
H7
ARPE
TERT
E
Firefly/Renilla
10
8
6
4
2
0
**
H7
HT1080
ARPE
H7 fib
F
ARPE
Firefly/Renilla
8
6
4
2
0
*
n.s.
EV
RE1
RE2
RE3
RE4
RE5
RE6
RE7
RE8
G
RE2
RE3
RE6
H1 H3K4me1
H1 H3K27ac
Refseq
RE2
RE3
RE6
CTD-3080P12.3
H
H1 H3K4me3
H9 H3K4me3
BJ H3K4me3
IMR90 H3K4me3
TERT

Figure S1. Identification of *hTERT* cis REs. **Related to Figure 1**. **(A)** RT-qPCR for hTERT levels in H7 human ESCs and in mortal human BJ fibroblasts. **(B)** Schematic of 1.1kb "fragend" containing the *hTERT* promoter defined by DpnII and Csp6I cut sites used in 4C experiment. **(C)** 4C-seq analysis derived from embryonic stem cells (H7, blue) and epithelial cells (ARPE, red) demonstrating the logarithmic decay of signal away from *hTERT* transcription start site (bait). **(D)** ATAC-seq profile from H7 ESC (blue) and ARPE (red) cells centered around hTERT promoter region. **(E)** Bar graph depicting the ratio of Firefly to Renilla luciferase activity driven by *hTERT* core promoter in the indicated cell lines (n=3 biological replicates, statistics calculated using student's t-test). ESCs display the highest baseline of hTERT promoter activity while mortal cell lines, including ARPE and differentiated fibroblasts, have low baseline activity. **(F)** Bar graph of Firefly to Renilla luciferase signal elicited when reporters carrying the indicated putative REs were transfected into ARPE cells (n=3 biological replicates, statistics calculated using ANOVA with multiple comparisons to empty vector (EV) values). None of the putative REs resulted in a significant difference in the *hTERT* promoter activity in ARPE cells. **(G)** Signal-over-control tracks displaying ENCODE-database ChIP-seq data for canonical enhancer histone marks, H3K4me1 and H3K27ac, in H1 ESC cells at putative enhancers RE2 and RE3 (H3K4me1). Data submitted to ENCODE. **(H)** As a control for histone marks at *hTERT* promoter in pluripotent cells vs differentiated cells, we show signal-over-control tracks displaying ChIP-seq data for H3K4me3, in the indicated cells types. Data from ENCODE.

Figure S2

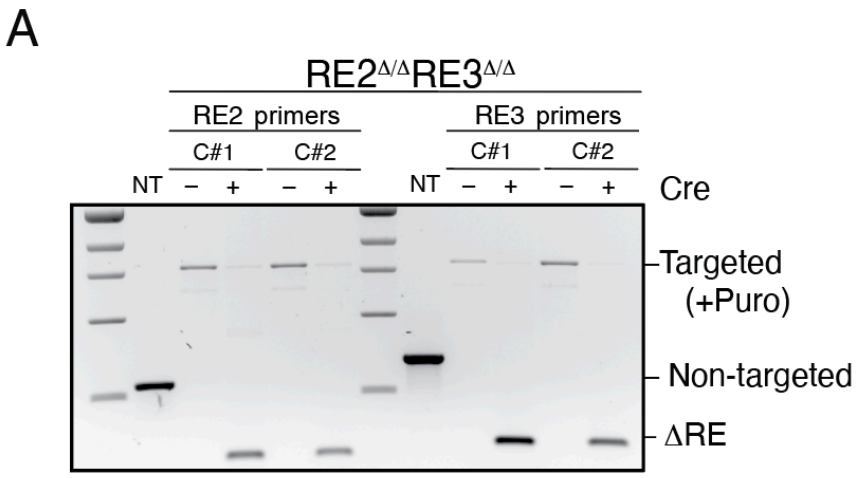

Figure S2. Deletion of *hTERT* enhancers reduce telomerase expression in embryonic stem cells. Related to Figure 2. **(A)** Genotyping PCR on RE2 and RE3 DKO cells with the indicated Cre-treatment and primers. PCR products (RE2/RE3): wild type, 560/700bp; targeted, 1500/1700bp and null alleles, 250/300bp.

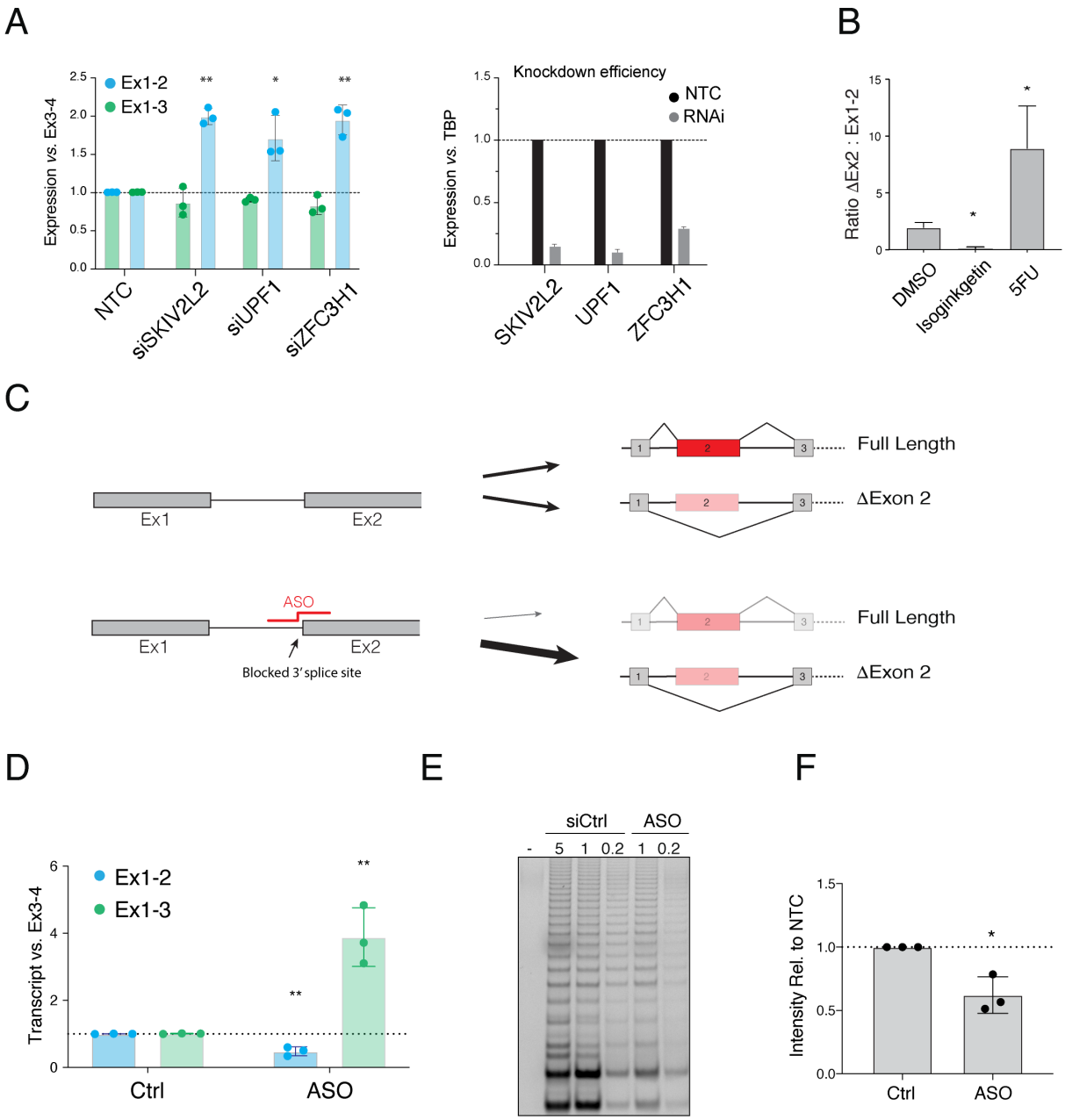

Figure S3. Characterization of *hTERT* ΔExon2 splice variant in somatic *vs.* pluripotent cells. Related to Figure 3. **(A)** Left: Quantification of *hTERT* exon1-2 and exon1-3 splice-junctions normalized to non-alternatively-spliced junction, exon3-4, in HeLa cells upon knockdown of the RNA decay factors, SKIV2L2, ZFC3H1 and UPF1. Depletion of these factors in Hela cells increases abundance of exon1-3 splice junctions while abundance of *hTERT* exon1-2 junctions are largely unaffected (n=3 biological replicates, *:p<0.05, **:p<0.01, statistics

calculated using ANOVA with multiple comparisons to NTC values). Right: efficiency of decay factor depletion by RNAi in Hela by qPCR. **(B)** Quantification of the abundance of hTERT-ΔEx2 relative to hTERT full-length using quantitative RT-PCR in ARPE treated with isoginkgetin (general pre-mRNA splicing inhibitor), 5-fluorouracil (RNA decay inhibitor), and DMSO control. Inhibition of global splicing decreased the ratio of hTERT-ΔEx2 to full-length. On the other hand, inhibition of RNA decay increased the ratio of hTERT ΔEx2 to full-length (n=3 biological replicates, $p<0.05$, statistics calculated using student's t-test comparing each condition to DMSO control). **(C)** Schematic illustration of anti-sense oligo (ASO) used to block the 3' splice site and inhibit the binding of the splicing machinery to hTERT transcript. **(D)** Quantification of hTERT exon1-2 and exon1-3 splice-junctions in HeLa cells following transfection with ASO. Transfection of HeLa with a splice-blocking ASO reduces the abundance of exon1-2 splicing and increases exon1-3 splicing abundance (n=3 biological replicates, $p<0.01$, statistics calculated using student's t-test). **(E)** Representative TRAP assay to detect telomerase activity in HeLa cells with the indicated treatment, with 5000, 1000 and 200 cell dilutions shown. **(F)** Graph depicting the quantification of the TRAP assay in **(E),** only 1000 cell dilution was used for quantification of signal intensity (n=3 biological replicates, $p<0.05$, statistics calculated using student's t-test).

Figure S4

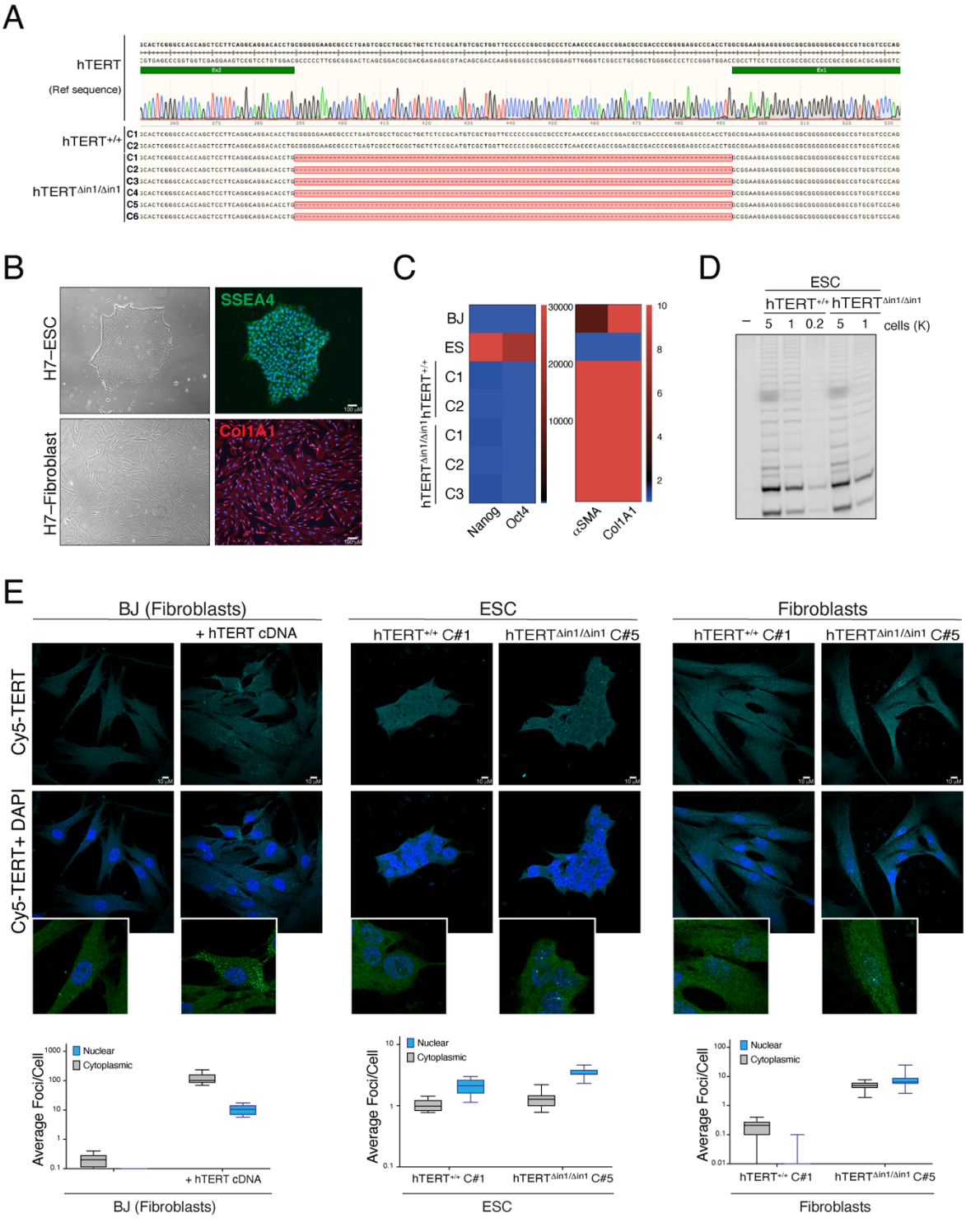
A
hTERT
(Ref sequence)
hTERT+/+
hTERTΔin1/Δin1
B
H7–ESC
H7–Fibroblast
SSEA4
Col1A1
C
BJ
ES
hTERT+/+
hTERTΔin1/Δin1
C1
C2
C3
Nanog
Oct4
αSMA
Col1A1
D
ESC
hTERT+/+
hTERTΔin1/Δin1
cells (K)
E
BJ (Fibroblasts)
+ hTERT cDNA
ESC
Fibroblasts
Cy5-TERT
Cy5-TERT+ DAPI
Nuclear
Cytoplasmic
Average Foci/Cell

Figure S4. Characterization of *hTERT*$^{\Delta in1/\Delta in1}$ ESCs and differentiated fibroblasts. Related to Figure 4. **(A)** Sanger sequencing of two hTERT$^{+/+}$ and six independent *hTERT*$^{\Delta in1\Delta in1}$ clones. Tracks aligned to reference genome sequence in Snapgene, **(B)** Brightfield images (left) and immunofluorescence images (right) of hESCs (top) and ESC-derived fibroblasts (bottom). ESCs have expected morphology and express the pluripotency-associated cell-surface marker, SSEA4. Differentiated fibroblasts express Col1a1, a marker of differentiated fibroblasts. **(C)** Heatmap of RT-qPCR data from differentiated fibroblasts of two *hTERT*$^{+/+}$ and three *hTERT*$^{\Delta in1/\Delta in1}$ clones. H7 ESCs and BJ fibroblasts were used as pluripotent and differentiated controls, respectively. *hTERT*$^{\Delta in1/\Delta in1}$ and *hTERT*$^{+/+}$ fibroblasts downregulate pluripotency genes (Oct4 and Nanog) and upregulate fibroblast identity genes (Col1a1 and αSMA) to a similar extent. Values are normalized to BJ fibroblast expression (n=3 biological replicates, $p<0.001$, statistics calculated using ANOVA with multiple comparisons to expression values for BJ fibroblast). **(D)** Representative TRAP assay indicates that *hTERT*$^{\Delta in1/\Delta in1}$ ESCs have comparable telomerase activity to hTERT$^{+/+}$ ESCs, dilutions shown for 5000, 1000, and 200 cells shown. **(E)** Top: Representative images of hTERT-specific smiRNA-FISH. Bottom: quantification of cytoplasmic and nuclear foci in the indicated cell types: mortal BJ fibroblasts (n=55), hTERT-immortalized BJ (n=91), *hTERT*$^{+/+}$ ESCs (n=163), *hTERT*$^{\Delta in1/\Delta in1}$ ESCs (n=255), *hTERT*$^{+/+}$ fibroblasts (n=94), and *hTERT*$^{\Delta in1/\Delta in1}$ fibroblasts (n=91).

Figure S5

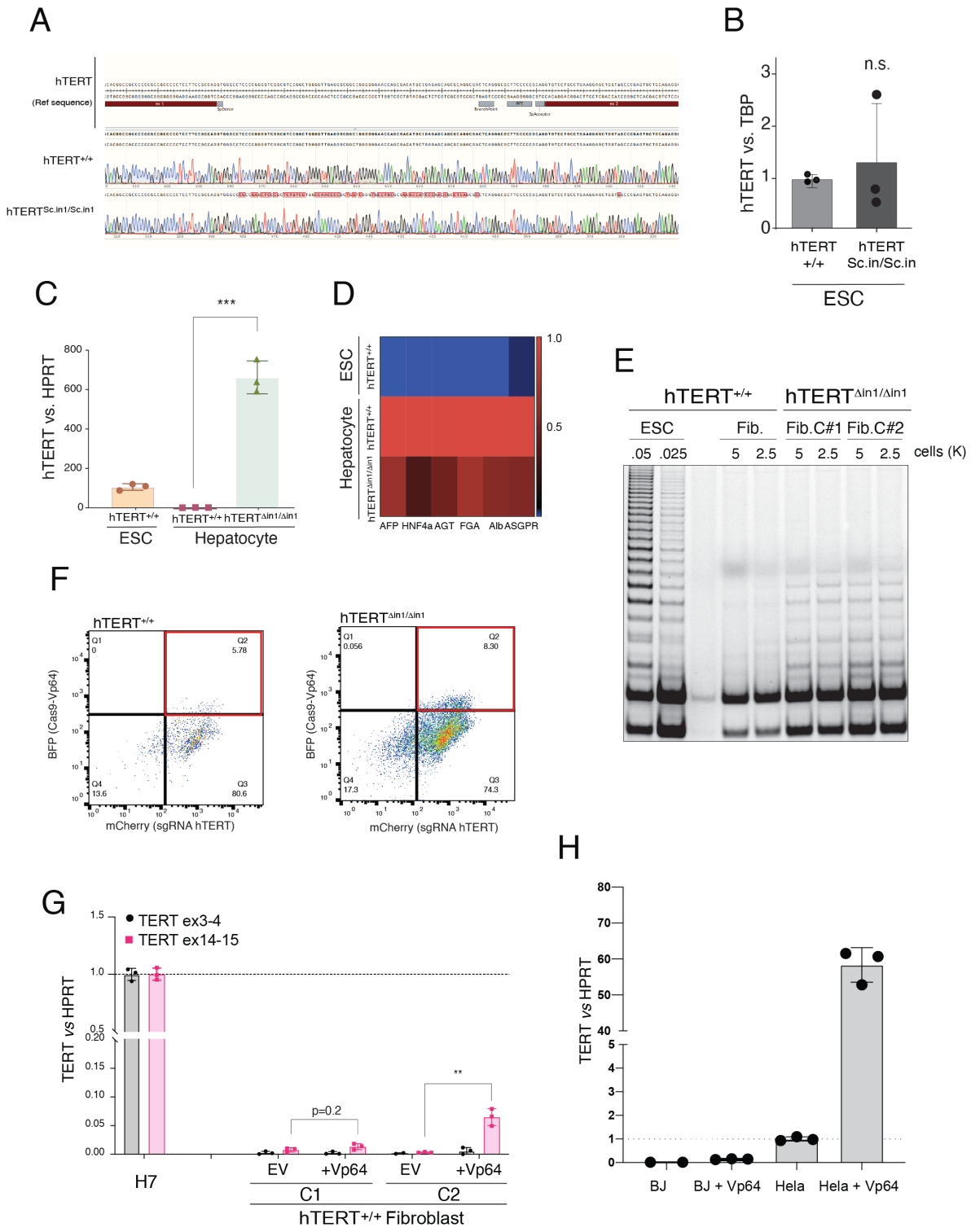

Figure S5. *hTERT*$^{\Delta in1/\Delta in1}$ cells fail to silence *hTERT*. Related to Figure 4. (A) Sanger sequencing of hTERT$^{+/+}$ and hTERT$^{Sc.in1/Sc.in1}$ cells (Sc.in1=scrambled intron 1). Tracks aligned to

reference genome sequence in Snapgene. Scrambled intron sequence has same base composition as WT intron but with randomly arrange nucleotides and conserved sequences required for splicing, T>G mutation in exon-2 was used to ablate PAM site and is a silent substitution. **(B)** Quantitative RT-qPCR for *hTERT* mRNA in ESCs with the indicated genotype. *hTERT* expression is similar in $hTERT^{Sc.in1/Sc.in1}$ ESCs and wildtype ESCs, indicating that *hTERT* intron-1 does not contain a transcriptional silencer. Values are normalized to those obtained from $hTERT^{+/+}$ differentiated hepatocytes (n=3 biological replicates, n.s., statistics calculated using student's t-test). **(C)** Quantitative RT-PCR for hTERT mRNA in cells with the indicated genotype during *in-vitro* hepatocyte differentiation (Mallanna and Duncan, 2013). *hTERT* expression is silenced in hepatocytes derived from wildtype H7 ESC clones, whereas, hTERT levels remains elevated upon differentiation of $hTERT^{\Delta in1/\ \Delta in1}$ ESCs into hepatocytes. Values are normalized to those obtained from $hTERT^{+/+}$ differentiated hepatocytes (n=3 biological replicates, $p<0.001$, statistics calculated using student's t-test for indicated pairs). **(D)** Heatmap of RT-qPCR data from differentiated hepatocytes obtained from $hTERT^{+/+}$ and $hTERT^{\Delta in1/\ \Delta in1}$ clones. H7 ESCs are used as pluripotent cell control. $hTERT^{\Delta in1/\ \Delta in1}$ and $hTERT^{+/+}$ hepatocytes upregulate early hepatic endoderm genes (AFP and HNF4a), mid-development hepatocyte genes (AGT and FGA) and mature hepatocyte genes (Albumin and ASGPR) to a similar extent. Values are normalized to those obtained from $hTERT^{+/+}$ differentiated hepatocytes (n=3 biological replicates, $p<0.001$, statistics calculated using ANOVA with multiple comparisons to $hTERT^{+/+}$ fibroblast values). **(E)** Representative TRAP assay to detect telomerase activity in cells with the indicated genotype. The TRAP confirms that $hTERT^{\Delta in/\Delta in1}$ fibroblasts retain low-level telomerase activity while $hTERT^{+/+}$ fibroblasts silence telomerase completely, dilutions of 5000 and 2500 cells shown for fibroblasts and 50 and 25 cells for ESCs. **(F)** FACS plot indicative of Vp64-Cas9 expression (BFP) and sgRNA expression (mCherry) in cells with the indicated genotype upon transduction with the transcriptional activation system. **(G)** RT-qPCR for hTERT mRNA in differentiated fibroblasts upon addition of Vp64-Cas9 transcriptional activation of *hTERT* promoter. Two $hTERT^{+/+}$ clones were transduced with lentivirus encoding Vp64-dCas9 transactivation protein and 2 guide RNAs complementary to *hTERT* promoter. Following FACS selection of Vp64-dCas9 expressing cells, RT-qPCR was performed on non-transduced parental clonal lines (EV for empty vector) and Vp64-dCas9 expressing cells. Transcriptional activation of hTERT promoter does not robustly increase hTERT mRNA in $hTERT^{+/+}$ fibroblasts (n=3, $p=0.2$ and $p<0.01$). **(H)** RT-qPCR for hTERT mRNA in BJ fibroblasts and HeLa cells upon addition of Vp64-Cas9 transcriptional activation of hTERT promoter.

Figure S6

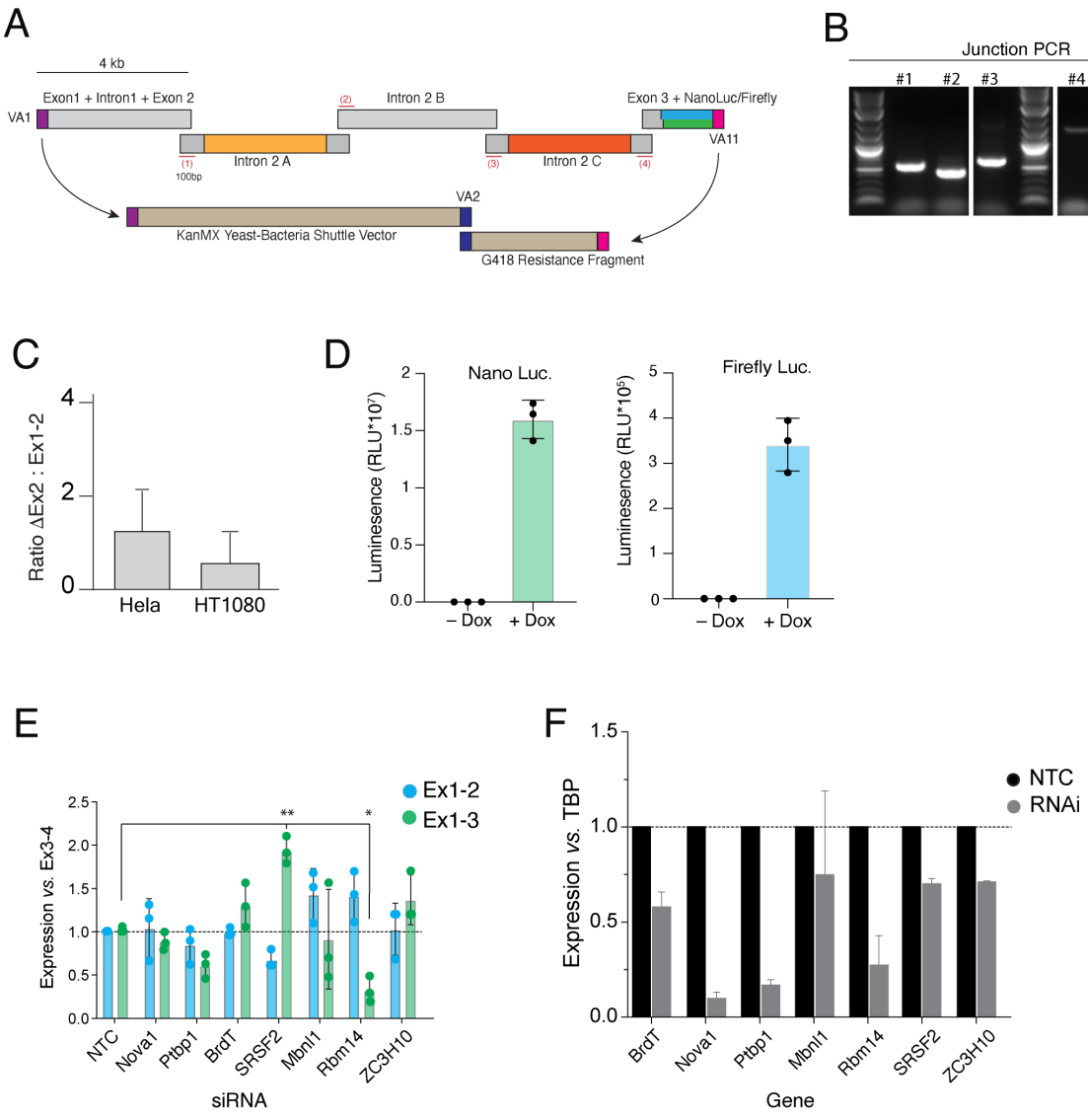
A
4 kb
Exon1 + Intron1 + Exon 2
VA1
(2)
Intron 2 B
Exon 3 + NanoLuc/Firefly
VA11
(1)
100bp
Intron 2 A
(3)
Intron 2 C
(4)
VA2
KanMX Yeast-Bacteria Shuttle Vector
G418 Resistance Fragment
B
Junction PCR
#1
#2
#3
#4
Neg.
C
Ratio ΔEx2 : Ex1-2
Hela
HT1080
D
Nano Luc.
Luminesence (RLU*10⁷)
– Dox
+ Dox
Firefly Luc.
Luminesence (RLU*10⁵)
E
Ex1-2
Ex1-3
Expression vs. Ex3-4
NTC
Nova1
Ptbp1
BrdT
SRSF2
Mbnl1
Rbm14
ZC3H10
siRNA
F
NTC
RNAi
Expression vs. TBP
Gene

Figure S6. Minigene reporter screen identifies positive and negative regulators of hTERT alternative splicing. Related to Figure 5. **(A)** Schematic illustration of mini-gene assembly by homologous recombination in yeast. Genomic locus for *hTERT* containing exons 1, 2, and 3 and intervening introns was amplified in 4kb amplicons that overlap by at least 100bp. Terminal fragments amended with VA1 and VA11 sequences to facilitate homologous recombination with yeast-bacteria shuttle backbone (KanMX) and Geneticin 418 resistance fragment. After selection for drug resistant colonies in yeast, minigene constructs were cloned into a mammalian expression vector. **(B)** PCR amplification across assembled junctions of *hTERT* minigene, confirming proper assembly of all 4 pieces in the appropriate order. **(C)** Quantification of the hTERT ΔEx2 to hTERT full-length ratio by RT-qPCR in two cancer cell lines, Hela and HT1080 (n=3 biological replicates). hTERT mRNA in HeLa cells display a ratio near 1:1 for hTERT ΔEx2 to hTERT full-length, indicating that the cell line would be suitable to detect any modulation in alternative splicing. **(D)** Quantification of luciferase signal from each reporter upon Dox induction in HeLa-FRT cell line heterozygous for each reporter construct. In each case, uninduced control wells were used to measure background luminescence and the measured background was subtracted (n=3 biological replicates, $p<0.0001$, statistics calculated by student's t-test). **(E)** Quantification of hTERT exon1-2 and exon1-3 splice-junctions normalized to non-alternatively-spliced junction, exon3-4, in HeLa cells upon knockdown of the indicated top-scoring RNA splicing factors from RNAi screen. Depletion of SRSF2 and RBM14 in Hela cells significantly changed abundance of exon1-3 and exon1-2 splice junctions. Other factors, including Nova1 and Ptbp1 that were previously showed to influence *hTERT* α/β splicing (Sayed et al., 2019), do not significantly alter hTERT exon-2 alternative splicing. (n=3 biological replicates, *: $p<0.05$, **: $p<0.01$, statistics calculated using ANOVA with multiple comparisons to NTC values). **(F)** Efficiency of decay factor depletion by RNAi in Hela in **(E)** by qPCR.

Figure S7

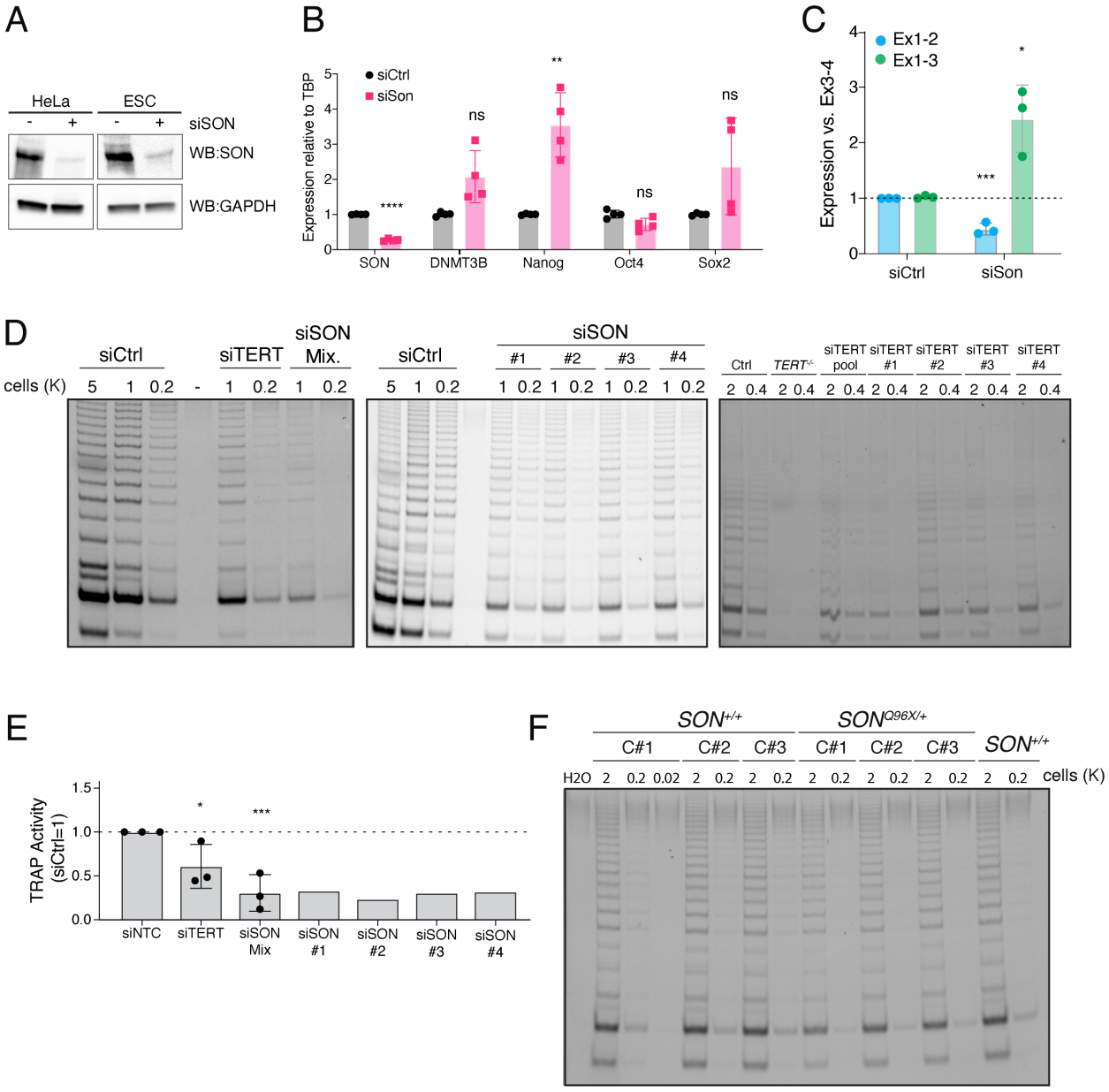
A
HeLa
ESC
siSON
WB:SON
WB:GAPDH
B
siCtrl
siSon
Expression relative to TBP
SON
DNMT3B
Nanog
Oct4
Sox2
ns
C
Ex1-2
Ex1-3
Expression vs. Ex3-4
siCtrl
siSon
D
siCtrl
siTERT
siSON Mix.
siSON
#1
#2
#3
#4
cells (K)
Ctrl
TERT-/-
siTERT pool
E
TRAP Activity (siCtrl=1)
siNTC
siTERT
siSON Mix
F
SON+/+
SONQ96X/+
C#1
C#2
C#3
H2O
cells (K)

Figure S7. SON regulates *hTERT* splicing as a function of pluripotency. Related to Figure 6. **(A)** Western blot to detect SON levels 48 hours post-transfection of HeLa and human ESCs with siSON (4-oligo pool) and siCtrl (non-targeting control siRNA). **(B)** Quantification of pluripotency factor (Oct4, Sox2, Nanog, Dnmt3B) and SON mRNA abundance in SON depleted human ESCs by RT-qPCR. Graph depicts a reduction in total SON transcript in human ESCs upon SON knockdown (n=3 biological replicates, $p<0.0001$, statistics calculated using student's t-test). At this time point, we detect no reduction in pluripotency associated genes (n=3 biological replicates, Oct4 $p=0.08$, statistics calculated using student's t-test comparing RNAi expression to that of siCtrl for each gene). **(D)** Representative TRAP assay to detect telomerase activity in HeLa cells, 48 hours after SON depletion with siRNA pool (Mix) or individual siRNAs. **(E)** Quantification of the TRAP assay as in **(D)**, only 1000 cell dilution was quantified for signal intensity. SON depletion results in a significant reduction in telomerase activity (n=3 biological replicates, *: $p<0.05$, ***: $p<0.001$, statistics calculated using ANOVA with multiple comparisons to siNTC signal intensity values). siSon Mix represents a pool of 4 independent siRNAs. In addition, we tested each siRNA individually in a single experiment (n=1). **(F)** Representative TRAP assay to detect telomerase activity in human ESCs with the indicated genotype. Lanes quantified were those comprising 2000 cells.

Supplemental table 1: List of RNA-binding proteins and splicing factors tested in RNAi screen related to Figure 5B.

AAR2	CWC15	GTF2F1	METTL16	PRMT5	RNF113B	SNU13	TXNL4B
ACIN1	CWC22	GTF2F2	METTL3	PRMT7	Rnf219	SNUPN	U2AF1
AFF2	CWC25	HABP4	MFAP1	PRPF18	RNPC3	SNW1	U2AF1L4
AHNAK	CWC27	HMX2	MPHOSPH10	PRPF19	RNPS1	SON	U2AF2
AHNAK2	CWF19L1	HNRNPA0	MYOD1	PRPF3	RP9	SREK1	U2SURP
AKAP17A	CWF19L2	HNRNPA1	NCBP1	PRPF31	RPS13	SREK1IP1	UBL5
AKAP8L	DAZAP1	HNRNPA1L2	NCBP2	PRPF38A	RPS26	SRPK1	UPF3B
AKT2	DBR1	HNRNPA2B1	NOL3	PRPF38B	RRAGC	SRPK2	USB1
ALYREF	DCPS	HNRNPA3	NONO	PRPF39	RRP1B	SRPK3	USP39
AQR	DDX1	HNRNPC	NOVA1	PRPF4	RSRC1	SRRM1	USP4
ARL6IP4	DDX17	HNRNPD	NOVA2	PRPF40A	RTCB	SRRM2	USP49
BCAS2	DDX20	HNRNPF	Npm1	PRPF40B	SAP18	SRRM4	WBP11
BRDT	DDX23	HNRNPH1	NSRP1	PRPF4B	SART1	SRRT	WBP4
BUD13	DDX39A	HNRNPH2	NUDT21	PRPF6	SART3	SRSF1	WDR33
BUD31	DDX39B	HNRNPH3	NUP98	PRPF8	SCAF1	SRSF10	WDR77
C1QBP	DDX41	HNRNPK	PABPC1	PRX	SCAF11	SRSF11	WDR83
C2orf49	DDX42	HNRNPL	PABPN1	PSIP1	SCAF8	SRSF12	WT1
C9orf78	DDX46	HNRNPLL	PAPOLA	PTBP1	SCNM1	SRSF2	WTAP
CACTIN	DDX47	HNRNPM	PCBP1	PTBP2	SETX	SRSF3	XAB2
CASC3	DDX5	HNRNPR	PCBP2	PTBP3	SF1	SRSF4	YBX1
CCAR1	DHX15	HNRNPU	Pcbp4	PUF60	SF3A1	SRSF5	YTHDC1
CCAR2	DHX16	HNRNPUL1	PCF11	QKI	SF3A2	SRSF6	ZBTB7A
CD2BP2	DHX35	HSPA1A	PDCD7	RALY	SF3A3	SRSF7	ZBTB8OS
CDC40	DHX38	HSPA8	PHF5A	RBFOX1	SF3B1	SRSF8	ZC3H10
CDC5L	DHX40	HTATSF1	PIK3R1	RBFOX2	SF3B2	SRSF9	ZC3H13

CDK12	DHX8	IK	PLRG1	RBFOX3	SF3B3	STH	ZCCHC8
CDK13	DHX9	ISY1	PNN	RBM10	SF3B4	STRAP	ZCRB1
CELF1	DNAJC8	IVNS1ABP	POLR2A	RBM11	SF3B5	SUGP1	ZMAT2
CELF2	DYRK1A	IWS1	POLR2B	RBM15	SF3B6	SUGP2	ZMAT5
CELF3	ECD	JMJD6	POLR2C	RBM15B	SFPQ	SUPT6H	ZNF326
CELF4	EFTUD2	KDM1A	POLR2D	RBM17	SFSWAP	SYF2	ZNF638
CELF5	EIF4A3	KHDRBS1	POLR2E	RBM19	SLC39A5	SYMPK	ZNF830
CELF6	ELAVL1	KHDRBS2	POLR2F	RBM20	SLU7	SYNCRIP	ZPR1
CHERP	ELAVL2	KHDRBS3	POLR2G	RBM22	SMNDC1	TAF15	ZRANB2
CIR1	ERN1	KHSRP	POLR2H	RBM24	SMU1	TARDBP	ZRSR2
CIRBP	ESRP1	LGALS3	POLR2I	RBM25	SNIP1	TFIP11	RBM14
CLASRP	ESRP2	Lmntd2	POLR2J	RBM28	SNRNP200	TGS1	FUBP1
CLK1	FAM172A	LSM1	POLR2K	RBM3	SNRNP25	THOC1	CCDC130
CLK2	FAM98B	LSM10	POLR2L	RBM38	SNRNP27	THOC2	EWSR1
CLK3	FASTK	LSM2	PPARGC1A	RBM39	SNRNP35	THOC3	USP43
CLK4	FIP1L1	LSM3	PPIE	RBM4	SNRNP40	THOC5	PCBP3
CLNS1A	FMR1	LSM4	PPIG	RBM41	SNRNP48	THOC6	CCDC94
CLP1	FRG1	LSM5	PPIH	RBM42	SNRNP70	THOC7	RAVER2
COIL	FUS	LSM6	PPIL1	RBM4B	SNRPA	THRAP3	IGF2BP2
CPSF1	FXR1	LSM7	PPIL3	RBM5	SNRPA1	TIA1	RBPMS2
CPSF2	FXR2	LSM8	PPP1R8	RBM7	SNRPB	TMBIM6	RAVER1
CPSF3	GCFC2	LUC7L	PPP1R9B	RBM8A	SNRPB2	TRA2A	USP31
CPSF4	GEMIN2	LUC7L2	PPP2CA	RBMX	SNRPC	TRA2B	NCL
CPSF7	GEMIN4	LUC7L3	PPP2R1A	RBMX2	SNRPD1	TRPT1	IGF2BP3
CRNKL1	GEMIN5	MAGOH	PPP4R2	RBMXL1	SNRPD2	TSEN15	FUBP3
CSTF1	GEMIN6	MAGOHB	PPWD1	RBMXL2	SNRPD3	TSEN2	IGF2BP1

CSTF2	GEMIN 7	MBNL1	PQBP1	RBMXL 3	SNRPE	TSEN3 4	RBPMS
CSTF2 T	GEMIN 8	MBNL2	PRCC	RBMY1 F	SNRPF	TSEN5 4	PSPC1
CSTF3	GPATC H1	MBNL3	PRDX6	REST	SNRPG	TTF2	METTL 25
CTNNB L1	GPKO W	METTL14	PRKRIP1	RNF11 3A	SNRPN	TXNL4 A	FTO

Supplemental table 3: List of Antibodies used throughout the study. Related to STAR Methods

Primary Antibodies	**Host**	**Company**	**Catalogue**	**Dilution**
GAPDH (0411)	Mouse	Santa Cruz Biotech.	sc-47724	1:10000 (WB)
SSEA-4 (MC-813-70)	Mouse	R&D Systems	MAB1435	1:500 (IF)
COL1A1 (3G3)	Mouse	Santa Cruz Biotech.	sc-293182	1:500 (IF)
SON	Rabbit	Novus Biologicals	NBP1-88706	1:1000 (WB)
Secondary Antibodies	**Host**	**Company**	**Catalogue**	**Dilution**
Mouse IgG, HRP-linked whole Ab	Sheep	GE Amersham	NA931V	1:5000 (WB)
Rabbit IgG, HRP-linked whole Ab	Donkey	GE Amersham	NA934V	1:5000 (WB)
Alexa Fluor 488 (D-anti-M)	Donkey	Life Technologies	A-21202	1:500 (IF)
Alexa Fluor 568 (D-anti-M)	Donkey	Life Technologies	A-10037	1:500 (IF)